Full Paper

Wiley Online Library

ELECTROANALYSIS

DOI: 10.1002/elan.202060322

Borohydride Reduction Method for PdIn/C Electrocatalysts Synthesis towards Glycerol Electrooxidation under Alkaline Condition

Júlio Nandenha,[a] Carlos Eduardo Domingues Ramos,[a] Sirlane G. da Silva,[a] Rodrigo Fernando Brambilla de Souza,[a] Eric Hossein Fontes,[a] Cristiane Angélica Ottoni,*[b, c] and Almir Oliveira Neto[a]

Abstract: Pd–In/C electrocatalysts were synthesized by the adapted borohydride reduction method in different atomic ratios. Electrocatalysts were evaluated by conventional electrochemical techniques and direct glycerol fuel cells. X-ray diffraction profiles indicated the structure of Pd and In (fcc) phases, as well as the presence of In higher oxidation states. Regarding Transmission electron microscopy, it showed the particle's average diameters between 6.1–12.7 nm. All PdIn/C electrocatalysts showed high current values for −0.30 V vs. Ag/AgCl, which the best one was PdIn/C 90:10. Higher performance for glycerol oxidation was observed in polarization curves at 90 °C for PdIn/C (30:70) composition.

Keywords: PdIn/C electrocatalysts · Direct alkaline fuel cell · Glycerol · electrooxidation reaction · polarization curves

1 Introduction

Glycerol represents a large bottleneck in biodiesel production [1]. In general, during the biodiesel production by transesterification process, 1 kg of waste product – glycerol – is produced for each 10 kg of fuel [2]. There is a particular interest in developing innovative technologies to use and valorize this waste [3] effectively. When analyzing glycerol's molecular structure, it contains three hydrated carbohydrates, which provide the potential for its application in energy production of fuel cells (FC) and the production of value-added by-products [4,5].

Electricity can be produced by low loads of glycerol [6]. That is why direct glycerol fuel cells (DGFC) have been gaining special attention compared to other direct liquid fuel cells. According to Pittayaporn *et al.* [7], DGFC operated under alkaline conditions can enhance glycerol oxidation and oxygen reduction reaction (ORR). Chino *et al.* [8] highlighted that the advantages of using DGFCs are that under alkaline conditions, a less corrosive environment is possible to be achieved as well as to use non-metallic nanoparticles. In agreement with Nascimento *et al.* [9], the scientific community has studied metallic nanoparticle synthesis and their use as active and selective catalysts for glycerol reactions in alkaline conditions, so it is essential to focus on the study of glycerol reactions aiming energy and products selective purposes.

Due to excellent catalytic activity in alkaline conditions, palladium-based (Pd) nanoparticles have extensively been studied for DGFC [10,11]. However, to improve the catalytic activity and reduce costs with the catalyst metal, new electrocatalysts should be designed with non-noble metals [12,13].

Asset *et al.* [14] synthesized Pd_xPb_{1-x} catalysts by the sacrificial support method (SSM). According to the authors, higher activities were obtained by ethylene glycol and glycerol oxidation using the composition $Pd_{0.77}$ $Pb_{0.23}$, when compared to Pd/C. Zalineeva *et al.* [15] also investigated glycerol's electrooxidation on Pd_xBi nanoparticles synthesized by the sacrificial support method. These authors were able to demonstrate an increase in glycerol oxidation reaction rate in the presence of bismuth (Bi). They found that bismuth promotes the current drop at higher potentials, caused by the slow kinetics of Pd surface oxide in Pd_xBi.

Some studies suggest that indium (In) is a potential element to be combined with platinum (Pt) or palladium (Pd). Recently, Cheng *et al.* [16] obtained PtIn/In_2O_3, Pt/In_2O_3, and Pt/C by the ethylene glycol (EG) method. PtIn/In_2O_3 has an excellent catalytic activity due to the electrons′ transfer from In to Pt and enhanced durability compared to Pt/C. Chen *et al.* [17] used In_3Pd_2 and In_3Pd_5 nanoparticles, improving the ethanol oxidation's catalytic performance in alkaline media, which was four times

[a] J. Nandenha, C. E. D. Ramos, S. G. da Silva, R. F. B. de Souza, E. H. Fontes, A. O. Neto
Instituto de Pesquisas Energéticas e Nucleares, IPEN/CNEN-SP, Av. Prof. Lineu Prestes, 2242 Cidade Universitária, CEP 05508-900 São Paulo, SP, Brazil
[b] C. A. Ottoni
São Paulo State University (UNESP) 11380-972 São Vicente, SP, Brazil
E-mail: cristiane.ottoni@unesp.br
[c] C. A. Ottoni
Instituto de Estudos Avançados do Mar (IEAMar), São Paulo State University, São Vicente/SP, Brazil

higher than commercial Pd/C catalysts. Those authors have shown that indium (In) incorporation significantly reduces the CO poisoning in Pd and Pt active sites. Santos *et al.* [18] have used the borohydride reduction method to obtain PtIn/C and they found that PtIn/C (70:30) exhibited higher performance for methanol oxidation in alkaline media compared to Pt/C.

Among all techniques described in the literature, the sodium borohydride method is faster, easier to operate, and cheaper. In this context, our group adapted this methodology for the preparation of Pd–In bimetallic nanoparticles supported on Vulcan carbon. The nanoparticles containing different amounts of In were characterized in morphology, crystalline structure, and electrochemical activity to improve DGFCs performance.

2 Material and Methods

Pd/C, In/C and PdIn/C electrocatalysts with atomic ratios of 90:10, 70:30, 50:50, and 30:70, with a fixed 20 wt.% metal loading was prepared by an adapted borohydride reduction method. In the adapted borohydride reduction (ABR). In ABR, metal sources of $(Pd(NO_3)_2 \cdot 2H_2O$, Fluka) and $InCl_3.xH_2O$ (indium chloride hydrate, Aldrich) were reduced at the same time. Briefly, carbon support and metal sources were dissolved in a mixture of water/2-propanol (50/50, v/v). The resulting mixture was submitted to an ultrasonic bath for 10 min. Finally, a sodium borohydride ($NaBH_4$, Aldrich) solution, used as a reducing agent, was added in one step, and this was maintained under continuous stirring for 30 min at room temperature. The resulting mixture was filtered, and all solids were washed with water and dried at 70 °C for two h.

X-ray diffraction (XRD) measurements were carried out using a diffractometer (Rigaku, model Miniflex II) with radiation (k = 0.15406 nm). The scanning angle was 2Θ from 20° to 90° with a step size of 0.05° and scan time of 2 s per step. Transmission electron microscopy (TEM) utilized a JEOL JEM-2100 microscope to estimate distribution and size for all electrocatalysts, where a particle distribution histogram was determined by measuring 150 particles.

Glycerol electrooxidation study was performed by cyclic voltammetry (CV) and chronoamperometry (CA); these measurements were carried out in a conventional three-electrode cell integrated to Autolab 302 N at room temperature [19]. The working electrodes were prepared using the thin porous coating technique, while the reference electrode was Ag/AgCl (3 $mol \cdot L^{-1}$ KCl), and the counter electrode was a Pt plate. CV (scan rate of 10mVs^{-1}) was performed using 1.0 $mol \cdot L^{-1}$ glycerol in a 1.0 $mol \cdot L^{-1}$ solution of KOH, saturated with N_2. Chronoamperometry experiments were performed using 1.0 $mol \cdot L^{-1}$ glycerol in a 1.0 $mol \cdot L^{-1}$ solution of KOH at −0.35 V for 1800 s.

Single direct glycerol fuel cell experiments were carried out using PdIn/C electrocatalysts in the anodes. It was used 2 $mg_{Pd} \cdot cm^2$ for each electrocatalyst, Nafion® 30 % (5 %, wt, Aldrich), ca Pt/C (BASF) electrocatalysts (2 mg_{Pd} cm^2), and Nafion® (30 %) in a single cell with an area of 5 cm^2. The electrodes were hot-pressed on both sides of a Nafion® 117 membrane, at 125 °C for 10 min, under a pressure of 100 $kgf \cdot cm^{-2}$. The temperature was set to 90 °C for glycerol in the fuel cell and 80 °C for the oxygen humidifier. Glycerol (2 $mol \cdot L^{-1}$) plus a 2 $mol \cdot L^{-1}$ KOH solution were delivered at a rate of 1 $mL \cdot min^{-1}$, and the oxygen flow was set to 150 $mL \cdot min^{-1}$. Polarization curves were obtained using a potentiostat/galvanostat (Autolab, model PGSTAT 302 N).

3 Results and Discussion

Figure 1 shows the X-ray diffraction patterns (XRD) through Bragg's peak for Pd and In supported on carbon. The formulations: PdIn (90:10, 70:30, 50:50 and 30:70) show the characteristics patterns of Pd (JCPDF # 87–643) at ≈39°, 45°, 67°, and 81° without relevant peak center displacement in comparison with Pd/C; this means that no insertion of In in the crystal lattice of Pd happened. The signal to noise ratio (SNR) is feeble, making it difficult to visualize the peaks; however, the formulations Pd: In 50:50, 70:30 and In/C have patterns of In-containing crystalline phases, such as the peak at 22° corresponding to In_2O_3 (JCPDF# 22–336). Pd: In (30:70) has three In phases at approximately 32°, 36°, and 40° corresponding to In^0 (JCPDF# 65–1172). Those peaks are expected since the 30:70 formulation has more In atoms exposed when is set side by side with other formulations. Finally, the 25° peak is associated with the carbon structure (002) of the carbon Vulcan XC-72. However, it should be noticed that still, In/C has an amorphous structure or small relative peak compared to Pd ones, Pd containing In clearly shows crystalline phases of In [1].

The micrographs and histograms of the particle size distribution obtained by TEM for PdIn/C with different atomic ratios are illustrated in Figure 2. The size of the

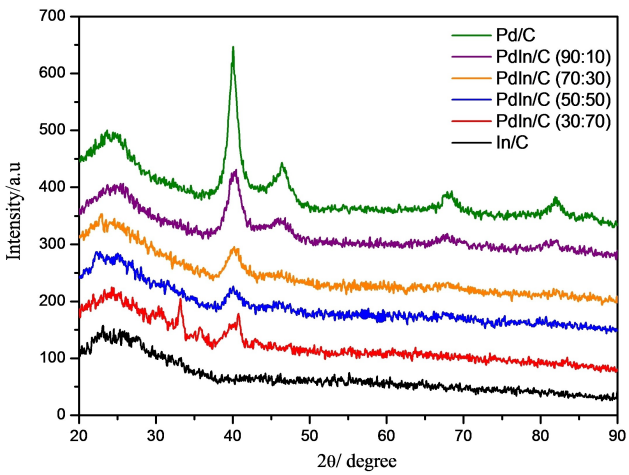

Fig. 1. XRD patterns of Pd/C and PdIn/C (90:10; 70:30; 50:50 and 30:70) electrocatalysts.

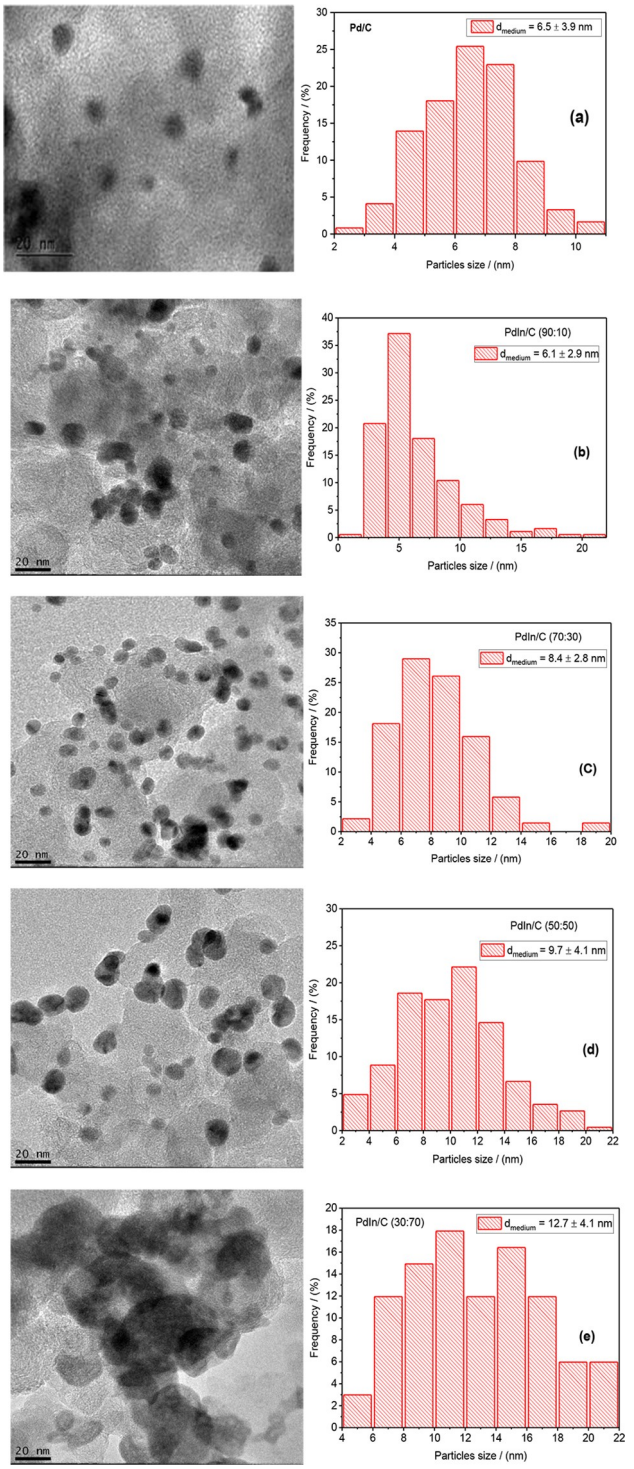

Fig. 2. TEM images and histograms of the particle size distribution for **(a)** Pd/C **(b)** PdIn/C 90:10, **(c)** PdIn/C 70:30, **(d)** PdIn/C 50:50 and **(e)** PdIn/C 30:70 electrocatalysts.

nanoparticles ranged between 6.1 and 12.7 nm. Furthermore, the addition of In to Pd promoted the growth and aggregation of the nanoparticles.

The CV of PdIn/C electrocatalysts is shown in Figure 3. All PdIn/C electrocatalysts synthesized show a well-

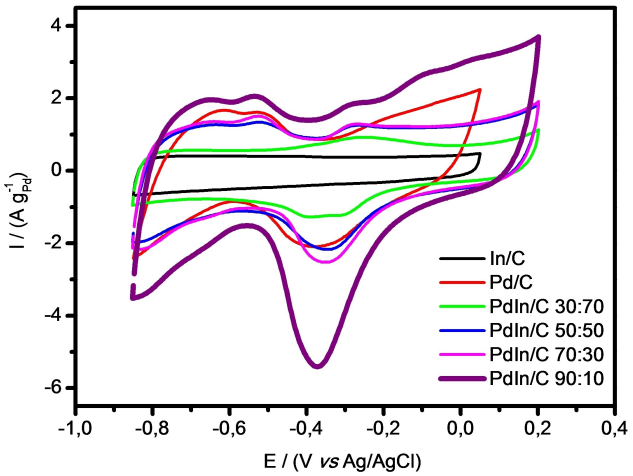

Fig. 3. Cyclic voltammograms of the In/C, Pd/C, and PdIn/C electrocatalysts in 1.0 mol·L^{-1} KOH solution with a sweep rate of 10 mV·s^{-1}.

defined hydrogen adsorption-desorption region (of −0.85 to −0.4 V vs Ag/AgCl) compared with In/C and PdIn/C 30:70 electrocatalysts. The voltammogram of PdIn/C 30:70 showed a suppressed hydrogen in the adsorption-desorption region, which indicates the partial coverage of Pd atoms by In. For PdIn/C 90:10, an increase in the current values in −0.35 to ~0.2 V was observed, indicating the abundance of oxide species [20,21,22]. The negative scan also showed an increase in the currents about −0.37 V (PdIn/C 90:10) associated with reducing oxide species [22,23,24].

Figure 4 shows the CV of the In/C, Pd/C, and PdIn/C electrocatalysts. All PdIn/C electrocatalysts showed high current values in −0.30 V in contrast to Pd/C and In/C. Hence, a beneficial effect of adding In to Pd is noticed. PdIn/C 90:10 showed the best performance in −0.5 V up to 0.2 V. Also, Pd/C showed higher currents regarding In/

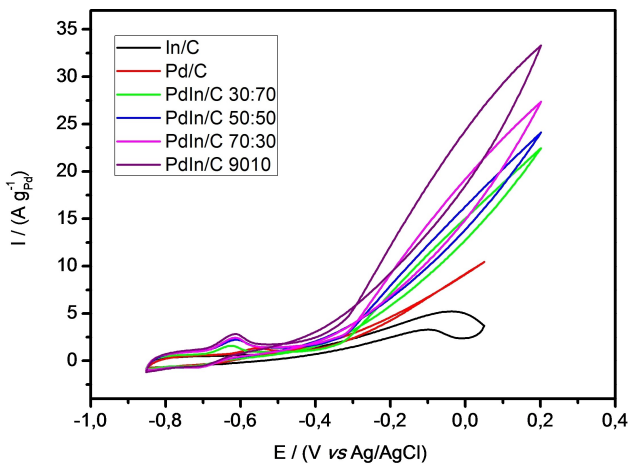

Fig. 4. Cyclic voltammograms of In/C, Pd/C, and PdIn/C electrocatalysts in 1.0 mol·L^{-1} glycerol in 1.0 mol·L^{-1} KOH solution with a sweep rate of 10 mV·s^{-1} at room temperature.

C for potentials above to −0.3 V. Moreover, PdIn/C 90:10 has the best electrochemical performance due to its smallest nanoparticle size compared to all other compositions; and also due to the synergistic effect between Pd and In [28].

The combined cyclic voltammograms and in-situ FTIR measurements detected glyceraldehyde at 1071 cm^{-1}, formate at 1225 cm^{-1}, and tartronate at 1345 cm^{-1}, glycerate at 1377 cm^{-1}, and carbonate at ~1405 cm^{-1}. Consequently, the glycerol oxidation reaction is following the mechanism proposed by [28]:

$$C_3H_8O_3 + 2H^+ + 2e^- \rightarrow C_3H_6O_3 \quad (1)$$

$$C_3H_6O_3 + 2H^+ + 2e^- + H_2O \rightarrow C_3H_5O_2O \quad (2)$$

$$C_3H_5O_2O^-4H^+ + 4e^- + H_2O \rightarrow COO^- - CHOH - COO- \quad (3a)$$

Or

$$C_3H_5O_2O^- + 2H^+ + 2e^- + H_2O \rightarrow C_2H_4O_2O- \quad (3b)$$

Or

$$C_3H_5O_2O^- + 2H^+ + 2e^- + H_2O \rightarrow HCOO^- \quad (3c)$$

$$HCOO^- + 2H^+ + 2e^- + \rightarrow COO^-O- \quad (4)$$

Figure 5 shows the chronoamperometry. The catalytic activities for all PdIn/C electrocatalysts were higher than for Pd/C, confirming that Pd′s activity and stability were improved with the co-presence of In. The current values obtained for PdIn/C 90:10 (2.90 A g_{Pd}^{-1}) were higher than those obtained for PdIn/C (70:30, 50:50, and 30:70) in agreement with cyclic voltammetry experiments. On the other hand, pure In/C electrocatalyst exhibits low activity.

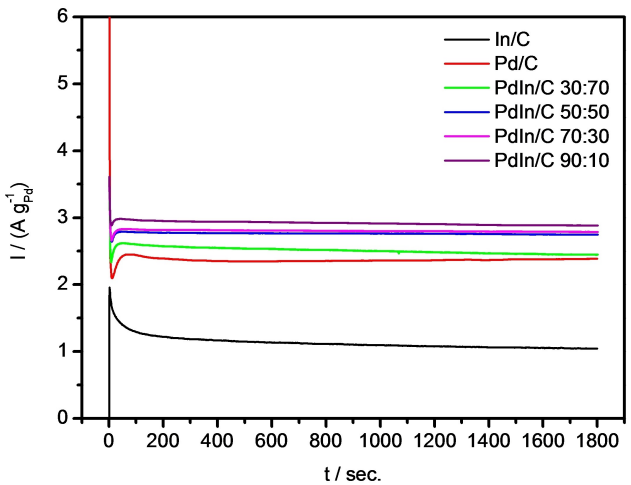

Fig. 5. Current-time curves at −0.35 V, in 1.0 mol·L^{-1} glycerol and a 1.0 mol·L^{-1} KOH solution, for In/C, Pd/C, and PdIn/C electrocatalysts at room temperature.

The electronic modification of Pd might be the possible reason for the enhanced catalytic activity [24,29].

The In/C, Pd/C, and PdIn/C activities were also evaluated in DGFC. The Pd/C and PdIn/C (30:70; 70:30 and 90:10) electrocatalysts showed similar open-circuit voltage (OCV), ~975 mV. The In/C and PdIn/C 50:50 electrocatalysts presented OCV values of 890 mV and 456 mV, respectively. PdIn/C 30:70 electrocatalysts presented the highest power density (22.65 mW cm^{-2}) as Figure 6a_2.shows; in contrast with PdIn/C (50:50) which shows the lowest performance (12.38 mW·cm^{-2}). These results could be understood in terms of the ohmic drop process. So, our methodology still needs further improvement regarding low main metal content. However, some of the PdIn prepared were more effective than Pd/C, indicating the beneficial effect of adding In to Pd following the classical electrochemical approaches used in this manuscript. This effect could be due to the improved

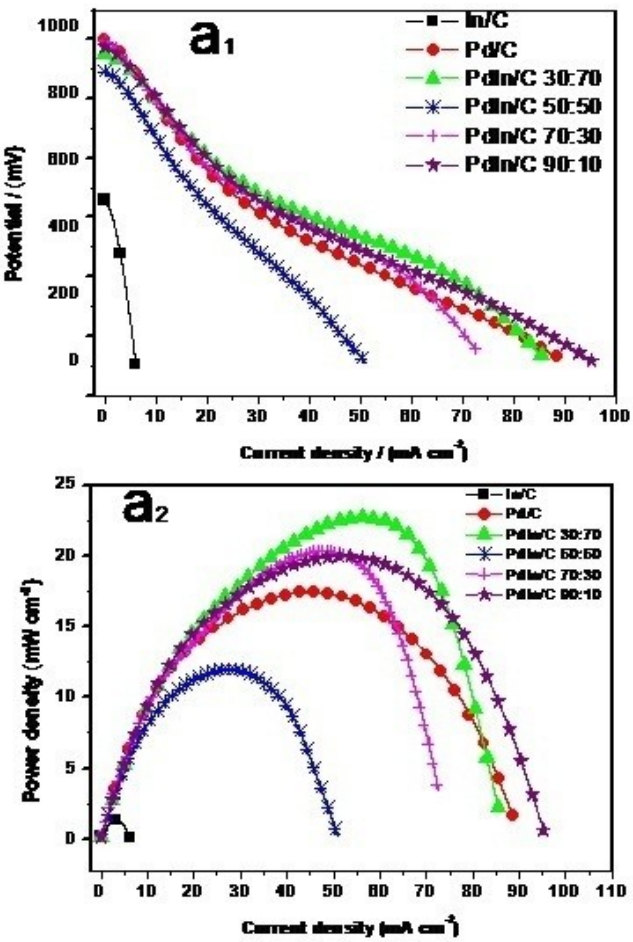

Fig. 6. Polarization **(a_1)** and power density curves **(a_2)** of a 5 cm^2 DGFC at 90 °C, using: In/C, Pd/C and PdIn/C electrocatalysts as anodic electrodes, Pt/C BASF electrocatalyst as cathodic electrode, fed with 2.0 mol·L^{-1} glycerol in a 2.0 mol·L^{-1} KOH solution. Anodic and cathodic catalytic were loaded with 1.0 mg·cm^{-2} of metal; Nafion® 117 membrane was used, and oxygen flux was set to 150 mL·min^{-1} at 85 °C.

kinetics reaction. However, the resistivity problem cannot be discarded. In/C showed a performance of 1.52 $mW \cdot cm^{-2}$, indicating that the use of In supported with carbon for the glycerol electrooxidation is not appropriate.

In DGFC performance studies, the following decreasing order of activity was observed: PdIn/C (30:70) > PdIn/C (70:30) ≈ PdIn/C (90:10) > Pd/C > PdIn/C (50:50) > In/C. The highest catalytic activity of PdIn/C 30:70 electrocatalyst, synthesized by the ABR, could also be attributed to chemisorbed oxygen species formation. They could promote the oxidation of adsorbed carbon monoxide on the surface of Pd (the bifunctional mechanism) [20–23].

The electrochemical experiments on the single DGFC [30–32] showed that the addition of In to Pd/C improved the glycerol electrooxidation just like the electrochemical experiments. However, both approaches could be different due to the distinct setup configurations, for example, different temperatures, other ohmic drops, and mass transport effects. However, electrochemical studies and fuel experiments showed that PdIn/C is more effective than Pd/C.

Ottoni *et al.* [30] showed that Pt-copper (Cu) electrocatalysts were better to oxidize glycerol using low Cu loading, and we have observed this same trend.

4 Conclusions

The sodium borohydride adapted reduction method was efficient to produce Pd/C, In/C, and PdIn/C electrocatalysts for glycerol electrooxidation. All the electrochemical measurements of PdIn/C showed the highest catalytic activity compared to Pd/C electrocatalyst. One possible reason could be the synergy between Pd and In atoms. The single DGFC showed that PdIn/C (30:70) is more effective than all other synthesized electrocatalysts. This optimum composition does not suppress the Pd active sites; instead, the DGFC performance is actually enhanced toward glycerol electrooxidation.

Finally, further studies still need to be done in order to avoid the ohmic drops in the fuel cell anodes, as well as to understand the electronic effect that In causes in Pd atomic structure.

Acknowledgements

The authors thank the IPEN/CCTM for the TEM measurements, FAPESP (2014/09087-4, 2014/50279-4, 2017/11937-4, 2017/21846-6 and 2017/22976-0) and CNPq (300816/2016-2 and 429727/2018-6) for the support.

Data Availability Statement

The authors confirm that the data supporting the findings of this study are available within the article [and/or] its supplementary materials.

References

[1] A. García-Trenco, A. Regoutz, E. R. White, D. J. Payne, M. S. P. Shaffer, C. K. Williams, *Appl. Catal. B* **2018**, *220*, 9.
[2] Y. Liu, W. Yu, D. Raciti, D. H. Gracias, C. Wang, *J. Phys. Chem. C* **2019**, *123*, 1426.
[3] L. Ji, F. Lei, W. Zhang, X. Song, J. Jiang, K. Wang, *Bioresour. Technol.* **2019**, *276*, 300.
[4] K. Yamamoto, A. M. Kiyan, J. C. Bagio, K. A. B. Rossi, F. D. Berezuk, M. E. Berezuk, *Green Process Synth* **2019**, *8*, 183.
[5] C. A. Martins, O. A. Ibrahim, P. Pei, E. Kjeang, *Chem. Commun.* **2019**, *54*, 192.
[6] H. Inoue, S. Kimura, Y. Teraoka, M. Chiku, E. Higuchi, B. T. X. Lam, *Int. J. Hydrogen Energy* **2018**, *43*, 18664.
[7] N. Pittayaporn, A. Therdthianwong, S. Therdthianwong, *J. Appl. Electrochem.* **2018**, *48*, 251.
[8] I. Chino, K. Hendrix, A. Keramati, O. Muneeb, J. L. Haan, *Appl. Energy* **2019**, *251*, 113323.
[9] A. A. Nascimento, L. M. Alencar, C. R. Zanata, E. Teixeira-Neto, A. P. M. Mangini, G. A. Camara, M. A. G. Trindade, C. A. Martins, *Electrocatalysis* **2019**, *10*, 82.
[10] I. Velázquez-Hernández, E. Zamudio, F. J. Rodríguez-Valadez, N. A. García-Gómez, L. Álvarez-Contreras, M. Guerra-Balcázar, N. Arjona, *Fuel* **2020**, *262*, 116556.
[11] N. Yahya, S. K. Kamarudin, N. A. Karim, M. S. Masdar, K. S. Loh, K. L. Lim, *Energ. Convers. Manage.* **2019**, *188*, 120.
[12] L. L. Carvalho, F. Colmati, A. A. Tanaka, *Int. J. Hydrogen Energy* **2017**, *42*, 16118.
[13] O. Muneeb, J. Estrada, L. Tran, K. Nguyen, J. Flores, S. Hu, A. M. Fry-Petit, L. Scudiero, S. Ha, J. L. Haan, *Electrochim. Acta* **2016**, *218*, 133.
[14] T. Asset, A. Serov, M. Padilla, A. J. Roy, I. Matanovic, M. Chatenet, F. Maillard, P. Atanassov, *Electrocatalysis* **2018**, *9*, 480.
[15] A. Zalineeva, A. Serov, M. Padilla, U. Martinez, K. Artyushkova, S. Baranton, C. Coutanceau, P. B. Atanassov, *J. Am. Chem. Soc.* **2014**, *136*, 3937.
[16] Y. Cheng, X. Zhao, Y. Yu, L. Chen, T. Cheng, J. Huang, Y. Liu, M. Harada, A. Ishihara, Y. Wang, *J. Power Sources* **2020**, *446*, 227332.
[17] Y.-J. Chen, Y.-R. Chen, C.-H. Chiang, K.-L. Tung, T.-K. Yeh, H.-Y. Tuan, *Nanoscale* **2019**, *11*, 3336.
[18] M. C. L. Santos, C. A. Ottoni, R. F. B. de Souza, S. G. da Silva, M. H. M. T. Assumpção, E. V. Spinacé, A. O. Neto, *Electrocatalysis* **2016**, *7*, 445.
[19] A. O. Neto, J. Nandenha, M. H. M. T. Assumpção, M. Linardi, E. V. Spinacé, R. F. B. de Souza, *Int. J. Hydrogen Energy* **2013**, *38*, 10585.
[20] A. O. Neto, J. Nandenha, R. F. B. De Souza, G. S. Buzzo, J. C. M. Silva, E. V. Spinacé, M. H. M. T. Assumpção, *J Fuel Chem Tech* **2014**, *42*, 851.
[21] P. S. Germain, W. G. Pell, B. E. Conway, *Electrochim. Acta* **2004**, *49*, 1775.
[22] C. A. Ottoni, C. E. D. Ramos, S. G. da Silva, E. V. Spinacé, R. F. B. de Souza, A. O. Neto, *Electroanalysis* **2016**, *28*, 2552.
[23] J. Nandenha, R. F. B. De Souza, M. H. M. T. Assumpção, E. V. Spinacé, A. O. Neto, *J. Int. Electrochem. Sci.* **2013**, *8*, 9171.
[24] A. N. Geraldes, D. F. Silva, J. C. M. Silva, R. F. B. Souza, E. V. Spinacé, A. O. Neto, M. Linardi, M. C. Santos, *J. Braz. Chem. Soc.* **2014**, *25*, 831.
[25] J. Ribeiro, D. M. dos Anjos, K. B. Kokoh, C. Coutanceau, J.-M. Léger, P. Olivi, A. R. de Andrade, G. Tremiliosi-Filho, *Electrochim. Acta* **2007**, *52*, 6997.

[26] J. Nandenha, R. F. B. De Souza, M. H. M. T. Assumpção, E. V. Spinacé, A. O. Neto, *Ionics* **2013**, *19*, 1207.
[27] M. Yovanovich, R. M. Piasentin, J. M. S. Ayoub, J. Nandenha, E. H. Fontes, R. F. B. de Souza, G. S. Buzzo, J. C. M. Silva, E. V. Spinacé, M. H. M. T. Assumpção, A. O. Neto, S. G. da Silva, *Int. J. Electrochem. Sci.* **2015**, *10*,104801.
[28] S. E. Mohamed, K. H. Hughes, A. Abdulgadir, S. Reza, L. Hanshuo, A. B. Gianluigi, E A Baranova, *ACS Sustainable Chem. Eng.* **2019**, *7*, 17.
[29] Y. Y. Feng, Z.-H. Liu, Y. Xu, P. Wang, W.-H. Wang, D.-S. Kong, *J. Power Sources* **2013**, *232*, 99.
[30] C. A. Ottoni, C. E. D. Ramos, R. F. B. de Souza, S. G. da Silva, E. V. Spinacé, A. O. Neto, *Int. J. Electrochem. Sci.* **2018**, *13*, 1893.
[31] N. Arjona, S. Rivas, L. Álvarez-Contreras, M. Guerra-Balcázar, J. Ledesma-García, E. Kjeang, L. G. Arriag, *New J. Chem.* **2017**, *41*, 1854.
[32] I. V. Hernández, M. Estévez, H. V. Castañeda, M. G. Balcázar, L. Á. Contreras, G. L. Bárcenas C Pérez, N. A. H. Pool, *Fuel* **2020**, *279*, 118505.

Received: July 7, 2020
Accepted: December 12, 2020
Published online on January 4, 2021

